J Solid State Electrochem (2012) 16:835–845
DOI 10.1007/s10008-011-1629-8

ORIGINAL PAPER

Overview of olivines in lithium batteries for green transportation and energy storage

K. Zaghib · A. Mauger · C. M. Julien

Received: 13 December 2011 / Accepted: 18 December 2011 / Published online: 19 January 2012

Abstract We present the progress on the physical chemistry of the olivine compounds since the pioneering work of Prof. John Goodenough. This progress has allowed $LiFePO_4$ to become the active cathode element of a new generation of Li-ion batteries that makes a breakthrough in the technology of the energy storage and electric transportation. This achievement is the fruit of about a decade of intensive research in the electrochemical community during which chemists, electrochemists, and physicists added there efforts to understand the properties of the material, to overcome the obstacles that were met on the way, and finally to reach the state of the art that allows its commercial use for worldwide applications in the industry today. These obstacles involved carbon coating, purification, control of the surface, the progressive decrease of the size of the particles down to nanoscale, and comprehensive investigation of surface effects. Nevertheless, heterogeneity in the quality of the product available on the market is damaging and may even be an obstacle to the development of new demanding technologies such as electric transportation. Emphasis is placed on the quality control that is needed to guarantee the reliability and the optimum electrochemical performance of this material as the active cathode element of Li-ion batteries. The route to increase the performance of Li-ion batteries with the other members of the family is also discussed. Since Prof. John Goodenough not only initiated the work but also played a major role in the research and development on these materials through the years, the present review is dedicated to him.

Keywords Olivine · Li-ion batteries · HEV, PEV, EV, energy storage

Contribution to the symposium: "The Origin, Development, and Future of the Lithium-Ion Battery", University of Texas at Austin, October 22, 2011

This paper is written in honor of Pr. John Goodenough.

K. Zaghib (✉)
Institut de Recherche d'Hydro-Québec (IREQ),
1800 Bd Lionel-Boulet,
Varennes, QC J3X 1S1, Canada
e-mail: zaghib.karim@ireq.ca

A. Mauger
Université Pierre et Marie Curie-Paris6, Institut de Minéralogie et Physique de la Matière Condensée (IMPMC),
4 place Jussieu,
75005 Paris, France

C. M. Julien
Université Pierre et Marie Curie-Paris6, Physicochimie des Electrolytes, Colloïdes et Sciences Analytiques (PECSA),
UMR 7195, 4 place Jussieu,
75005 Paris, France

Introduction

The story begins in 1834, when a German mineralogist, J.N. von Fuchs, discovered a mineral to which he gave the name triphylin, which is still the German name that has been translated as triphylite in English [1]. Its name comes from its chemical formula $Li(Fe^{2+},Mn^{2+})[PO_4]$, which has a Greek root, "tri" referring to the three cations in the formula as the solid solution $Li\ Fe_xMn_{1-x}PO_4$ exists in all proportions. To distinguish between them, triphylite refers to Fe-rich minerals while Mn-rich ones are called lithiophilite. For some time, this primary and rather rare mineral has interested only mineralogists, and the experiments focused for some time on its crystallographic structure, which is now part of the open database of the crystal structure of all the minerals. Still, $LiFePO_4$ without any manganese in it is only a product made in the laboratory, and its detailed structure dates from 1967 when Santoro and Newnham reported both its crystal structure from X-ray diffraction (XRD) and its magnetic structure from neutron diffraction [2]. Later investigations were still focused on the refined structure of the olivine type, including a

distorted hexagonal anion close packing [3]. Then, the material only interested gem collectors; and actually, as far as we know, only one paper has been published in the ninetieths before 1997 [4]. The rebound came in 1997 when J. Goodenough, proposed $LiFePO_4$ as a good candidate to be a cathode element for Li-ion batteries [5]. Indeed, the material is attractive. The crystal structure in Fig. 1 shows that the material is made of iron-oxygen (*bc*) planes, so that the material looks lamellar, giving some space in between to accommodate Li^+ ions. However, the planes are linked together by PO_4 bridges. Therefore, the material is really a three-dimensional compound, resulting in a remarkable thermal stability that the lamellar compounds miss, opening a route to Li-ion batteries much safer than before. Nevertheless, it still took about a decade before $LiFePO_4$ has won the market and asserted itself as the choice relevant to such demanding applications as electric vehicles. This rather long delay gives evidence of different obstacles that were met on the way before reaching the point where the material could be prepared in huge quantity with the high quality that guarantees the reproducibility of its electrochemical properties with a long calendar life. It is the purpose of this review to report on these difficulties, how they have been overcome, and their origin. The success of $LiFePO_4$ and the exponential increase in the needs for its production has resulted in a concomitant increase in the number of factories that produce $LiFePO_4$ throughout the world. Some of them, however, are not aware of the difficulties and traps that may damage the performance of this material. The consequence is an increasing heterogeneity in the quality of the product that is commercialized, depending on who is preparing it. The purpose of this work is not to make a benchmark and compare the different sources across the world. On the other hand, we hope that the report of the relationships between the defects (in the broad sense of the term) and their consequences on the properties will help manufacturers in their control of the quality of their product, which is crucial to the development of the Li-ion industry. This is one goal of this review. We also report on the most recent works that open new routes of research to increase the energy by using the other members of the family, as this is the main parameter that needs to be improved in the future, regarding the positive electrode of Li-ion batteries.

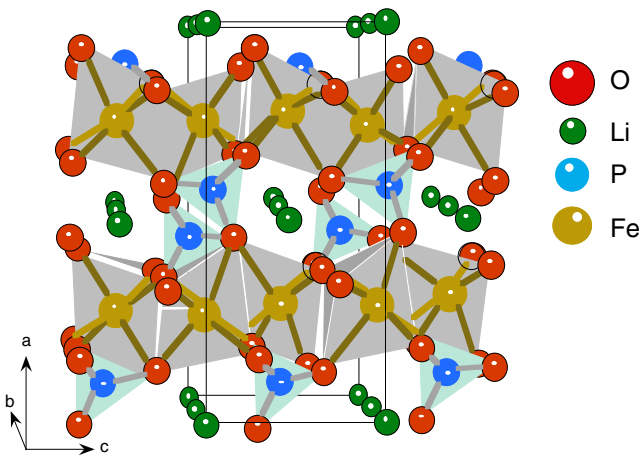

Fig. 1 Schematic representation of the olivine crystal structure of $LiFePO_4$. The iron-oxygen (*bc*) planes linked together by PO_4 bridges give space in between to accommodate Li^+ ions

Numerous synthesis routes are now available to prepare material of high quality. We have already reviewed them recently [6], which is why we do not report on this important aspect here and only refer to this work already published few months ago. Attention is thus focused hereunder on the structural and physical properties in relation to the electrochemical performance, irrespective of the synthesis route.

First problem: the low conductivity

The first difficulty that was encountered is the very poor electronic conductivity of $LiFePO_4$, which may result in losses in capacity even at moderate cycling rates. The intrinsic electrical resistivity has an activation energy that is about 0.65 eV [7]. This is not so large for an ionic material and actually is much smaller than the optical gap [8]. The reason is that the conductivity proceeds by a hopping process of small magnetic polarons. The polaron originates from a Li vacancy, which implies the presence of an iron ion in the +3 state by charge compensation. The spin of the hole on the Fe^{3+} ion is then coupled ferromagnetically by a double exchange mechanism to the Fe^{2+} ions in its vicinity, forming a ferromagnetic cloud, that can be detected by magnetic measurements [9]. This polaron hole, accompanied by its ferromagnetic cloud, can jump from the Fe^{3+} site to the neighboring Fe^{2+} site so that the Fe^{3+} and Fe^{2+} ions are exchanged. In this hopping process, in which the hole is in a bound polaron state with the same energy after and before the hop, the activation energy is simply the energy barrier that the hole has to overcome to jump to the next site. This is much less than the binding energy required to send a *d*-electron from an Fe^{2+} valence band to the conduction band, an energy of 0.65 eV that is typical of the hopping process in iron systems [10, 11]. Nevertheless, this activation energy is still too large, and thus the electronic mobility is too small, to envision the use of $LiFePO_4$ as a cathode for Li-ion batteries with bare particles. The way to overcome this problem was to add carbon, either by use of carbon additives to the $LiFePO_4$ matrix [5, 12], or by surface coating the $LiFePO_4$ particles with thin layers of carbon [13–15]. Fortunately, iron combines easily with carbon, so that different sources of carbon can be used and have been tested [16, 17]. Our experience is that lactose is a good precursor [18], although other choices are possible. The

carbon liberated from the lactose added to the precursors of $LiFePO_4$ in the course of synthesis increases the electronic conductivity by seven orders of magnitude. Figure 2 shows the resistivity curve of $LiFePO_4$ particles before and after carbon coating.

To achieve this result, however, the carbon needs to be conducting. This can be checked easily by Raman spectroscopy. The carbon leads to two characteristic bands in the Raman spectrum, named the D band and the G band at 1,345 and 1,583 cm^{-1}, respectively, when recorded using the 514.5-nm argon laser line. The shape of the bands, however, depends strongly on the kind of carbon. In particular, the growing up of the G band (G refers to graphite which is the most conductive form of carbon) at the expense of the D band means larger conductivity. The G and D bands are actually composed of more components, so that not only the intensity, but also the shape of the bands depends very much on the type of carbon that is deposited, and in particular on its conductivity [19]. This dependence has been extensively studied in the past, owing to the importance of carbon deposits in electronic devices, and it has been used to probe the carbon coat deposited on $LiFePO_4$ [17, 20]. In particular, a good estimate of the conductivity of the carbon layer can be done from an analysis of the Raman spectrum [21, 22]. As a result, illustrated in Fig. 3, the Raman spectrum is approximately that of coke, a conductive variety of carbon, provided the carbon coating has been performed at a temperature above 500 °C [21]. As the conductivity of the carbon increases with the temperature used for the coating process, higher temperatures have been explored. The limit

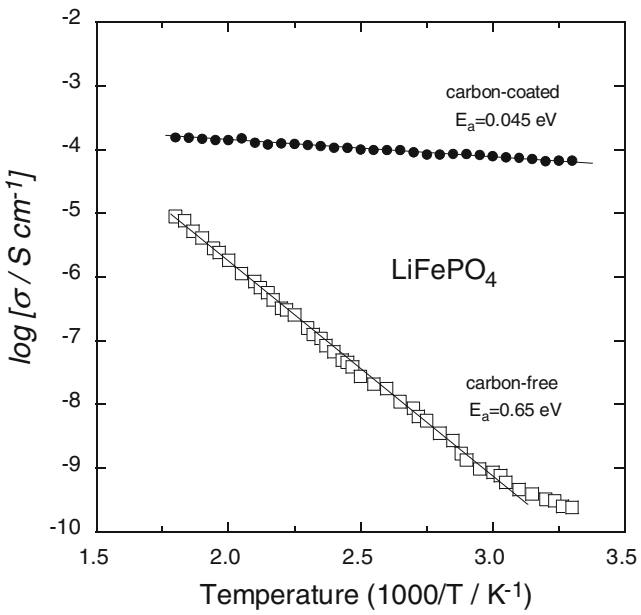

Fig. 2 Electric conductivity of $LiFePO_4$ particles before and after carbon coating (the size of the particles for this particular sample was 1 μm)

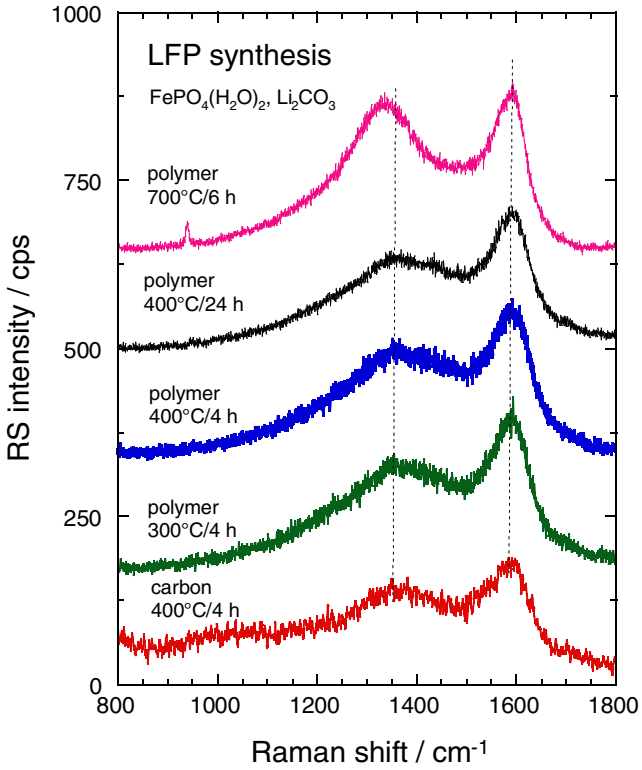

Fig. 3 Raman spectrum of C-$LiFePO_4$ showing the D and G bands of the carbon layer deposited at different temperatures indicated in the figure

comes from the partial decomposition, with the formation of secondary phases, at *circa* 800 °C. A systematic study as a function of the sintering temperature has shown that the optimum temperature is *circa* 650 °C [18].

With the carbon-coated particles referred as C-$LiFePO_4$, the mean free path of an electron inside a $LiFePO_4$ particle is limited to the radius of the particle. When an electron arrives at the surface of this particle, it can be driven to the collector of the electrode through the conductive carbon that forms a percolating network inside the powder. The electric conductivity on the path between the electron and the collector is now limited only by the average radius of one particle, which can be decreased to few tenths of nanometers, orders of magnitude smaller than the distance that separates the particle from the collector. That is the reason why the overall conductivity has been increased by orders of magnitude and the reason why, contrary to some recent claims [23], the coating is mandatory [6]. An illustration is given in Fig. 4, which compares the electrochemical performance of a sample before and after coating. The particles are small, 25-nm thick since the need for the carbon coating had been questioned especially for small particles [23]. As expected, the capacity is very small before coating and the full capacity is recovered after coating. Indeed, it is for smaller particles that the coating is most efficient, since it reduces the mean free path inside the insulating $LiFePO_4$ to the small radius of the particle.

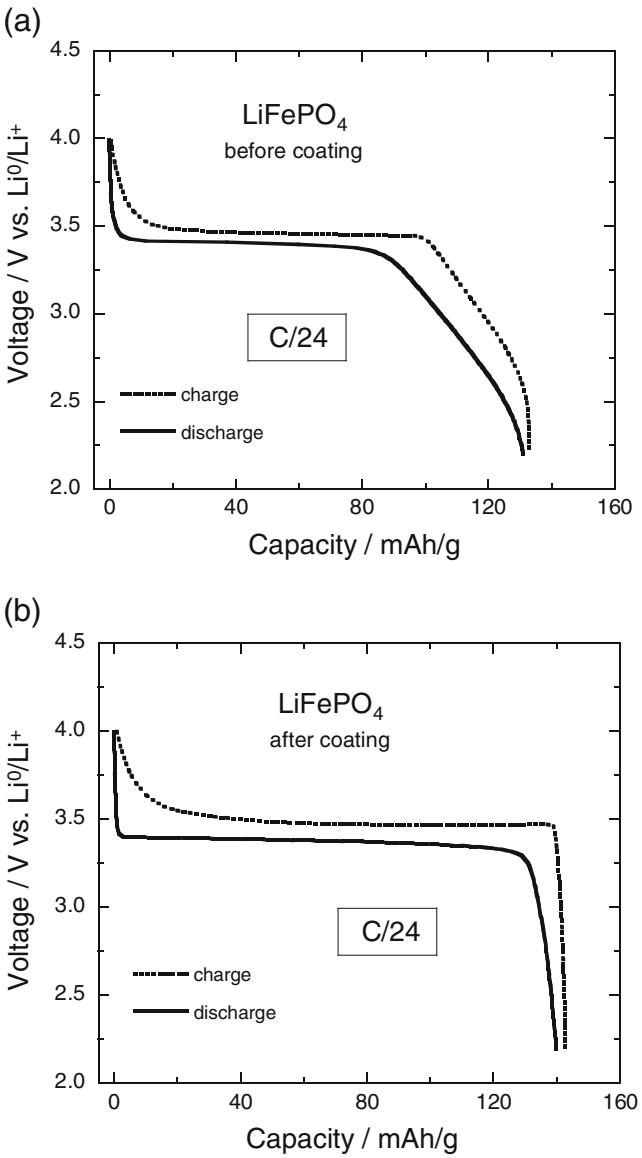

Fig. 4 Electrochemical performance of 25-nm thick $LiFePO_4$ particles before and after carbon coating, for comparison. Tests were carried out at C/24 rate

The carbon coating process has an indirect second beneficial effect that has only been understood more recently. The surface of the $LiFePO_4$ particles before carbon coating is usually made of a strongly disordered, 3 nm-thick surface layer that has been repeatedly observed by transmission electron microscopy (TEM) [24–26]. In situ TEM experiments have been performed to observe the evolution of the surface of the particles at the atomic scale during the coating process [18]. As a result, we have observed that the carbon coating is accompanied with the re-crystallization of the surface layer. The carbon itself helps, but actually, the crystallization is observed even in the absence of carbon precursor, i.e., without carbon coating. This result gives evidence that the re-crystallization is mainly the effect of annealing at 650 °C. This re-crystallization increases the ionic and electronic conductivity in the surface layer and is thus beneficial to the electrochemical properties.

Other attempts to improve the electronic conductivity include addition of dispersed metal powders [27]. In the same spirit, some attempts have been made to replace the carbon by an Fe-rich phosphoride metal, such as Fe_2P [28, 29]. On the one hand, although the presence of Fe_2P does increase the electronic conductivity, it also decreases the ionic conductivity so that both the capacity and cycling rates are degraded with respect to the carbon-coated $LiFePO_4$. But most of all, Fe_2P also has the disadvantage that it dissolves in the electrolyte, leading to the migration of iron to the anode of the Li-ion battery, which reduces dramatically the calendar life of the battery [30]. Another attempt to escape the carbon coating was to try doping. In particular, the claim that low-level doping by a range of aliovalent ions could increase the conductivity [31] has raised interest, although it was not proved [32]. However, in such ionic compounds as this olivine material, there is no hope to succeed to achieve a doping level on the Fe site high enough to have significant effect on the conductivity [9]. This has been confirmed by theoretical calculations of dopant substitution energies for cations that indicate supervalent doping on either Li or M sites is energetically unfavorable and does not result in an increase in electronic conductivity [33, 34]. Experimentally, evidence has been provided in [35] showing that the aliovalent ions reside primarily on the *M*1(Li) site. Moreover, the aliovalent ion charge is balanced by lithium vacancies, with the total charge on the iron site being exactly +2.000 not indicating enhanced electronic conductivity [35], so that the aliovalent ion is actually not a dopant. Instead, the location of the aliovalent ion within the lithium channels may hinder Li ion diffusion. Therefore, this attempt of doping is doomed to failure. The increase of conductivity wrongly attributed to doping in the past is due either to a carbon coating owing to the carbon that was present among the precursors [36], or the formation of a network of metal-rich phosphide [37], and again, it will reduce the calendar life by its dissolution in the electrolyte.

The conclusion of this section is thus that coating with conductive carbon is unavoidable. Independent of the size of the particles, carbon coating at *circa* 650 °C is mandatory and should be controlled to obtain a good $LiFePO_4$ product (i.e., a product that can be used to manufacture high-performance Li-ion batteries). This is the solution that overcomes the low intrinsic electrical conductivity and cures the structural disorder natively observed in the 3-nm thick surface layer of the particles.

Second problem: the impurities

Even after the carbon coating, which was systematic after year 2001 in most laboratories, the electrochemical properties of C-

$LiFePO_4$ lacked reproducibility, preventing its development by industry. The origin of this problem was the presence of impurities and defects that poisoned the material. As shown in Fig. 1, the lithium ions are located in the space left by the PO_4 units between the Fe–O layers in the (*bc*) planes. Yet the *b* and *c* directions are not equivalent, and the energy barrier that the Li has to overcome to move from one unit cell to the next one is 0.55 eV along the *b* direction, against 2.89 eV along the *c* direction [38]. In practice, the Li-ions will move along the path that costs a minimum of energy, so that they will slalom in the *b* direction [39]. The motion is then one dimensional. The consequence is that any impurity along this channel can block the channel, reducing the capacity. The electrochemical performance is thus very sensitive to any defect or impurity. In addition, these impurities influence the shape of nano-sized particles that are either amorphous and/or too small to be detected by X-ray analysis. The solution to detect the impurities is thus a combination of infrared spectroscopy and magnetic measurements. Fourier transform infrared spectroscopy (FTIR) probes the vibrations of the molecular edifices such as the PO_4^{3-} units at the molecular scale, so that only the short-range ordering matters: the method is sensitive, whether the impurities are crystallized or amorphous. The magnetic properties at the atomic scale probe the local environment of iron in a material where the magnetic interactions are short range.

Optical spectroscopy The FTIR absorption spectrum of $LiFePO_4$ is well known [40]. It is illustrated in Fig. 5. This spectrum was recorded with a Fourier transform interferometer (model Bruker IFS113v) in the wavenumber range 150–1,400 cm^{-1} at the spectral resolution of 2 cm^{-1}. The lines at 940–1,058 cm^{-1} are associated with ν_2 and ν_3 intra-molecular symmetric and asymmetric stretching modes of PO_4, respectively. The bands in the range 372–647 cm^{-1} are bending modes (ν_2 and ν_4) involving O–P–O symmetric and asymmetric modes and lithium vibrations. In between, there is a gap without any intrinsic band, so that any band detected in the range 700–900 cm^{-1} is the signature of an impurity. An example of the use that can be made of the FTIR spectroscopy to determine the impurities is given in Fig. 5. The spectrum has been recorded during the early stage of the crystallization of $LiFePO_4$ by solid-state reaction [41] after sintering at 400 °C for 4 h only. The spectrum has been recorded with the same apparatus as that of the pure and well-crystallized $LiFePO_4$ sample in the same figure so that direct comparison is possible.

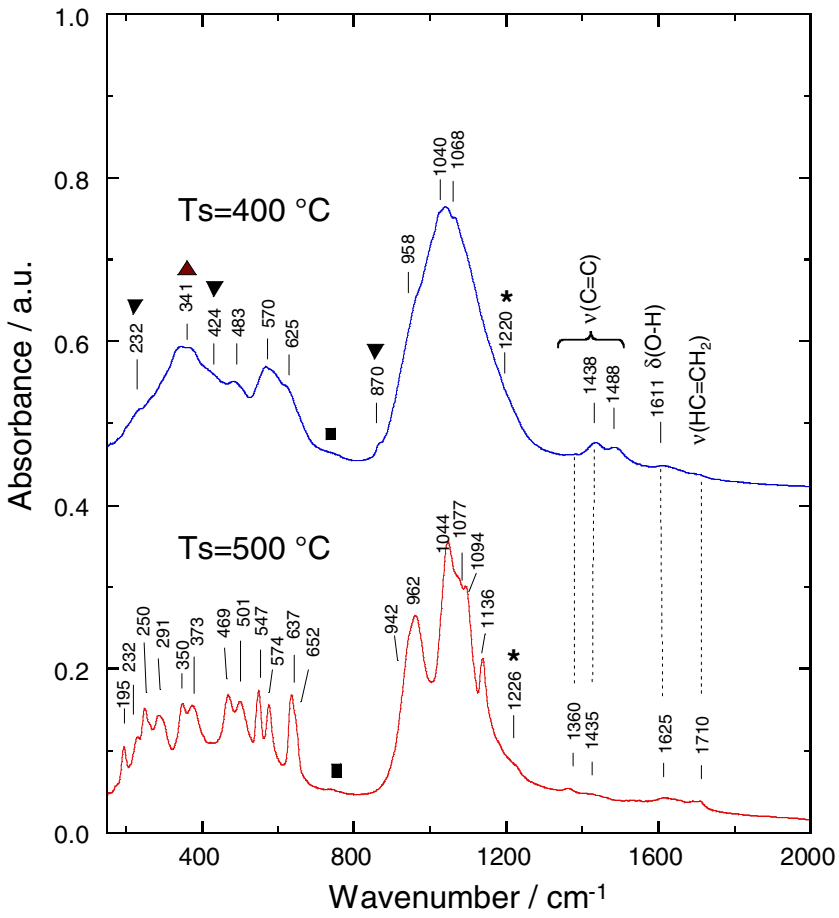

Fig. 5 FTIR spectra of well-crystallized $LiFePO_4$ free of impurity and $LiFePO_4$ at the early stages of the synthesis (sintering temperatures T_s=400 and 500 °C), with still different impurities and incomplete decomposition of the precursors. Extrinsic vibrations are marked by different symbols: $LiFeP_2O_7$ (*filled squares*), $Li_3Fe_2(PO_4)_3$ (*asterisks*), Li_3PO_4 (*filled inverted triangles*), $FePO_4$ (*filled triangles*). Other vibrations also identified in the figure -$HC{=}CH_2$ (vinyl group of the polymer), δ(O–H) (bending mode coming from the $FePO_4{\cdot}2H_2O$ precursor), the other bands are associated to ν(C–C) vibrations

First, the FTIR spectrum is broader than that of the spectrum of the sample prepared under the better conditions (sintering at 500 °C) in Fig. 5, because of the poorer crystallinity. However, the main result is the observation of new extrinsic modes. The band centered at 424 cm^{-1} is the signature of a small amount of lithium phosphate (Li_3PO_4). The new band centered at 741 cm^{-1} is the asymmetric ν_0 mode of P–O–P bridges of $LiFeP_2O_7$, which gives evidence of the presence of this impurity phase. The additional feature at 1,226 cm^{-1} is the signature of $Li_3Fe_2(PO_4)_3$, to which we refer in the following as NASICON. These are three main impurity phases that can be observed, depending on the mode of preparation. The other bands are not related to impurity phases formed during the sintering process. For instance, the extra bands in the spectral range above 1,300–1,600 cm^{-1} are ν(C–C) vibrations due to the remaining hydrocarbon species; the polymer that has been used as a precursor of the carbon has not been completely dissociated at the sintering temperature $T_s \approx 400$ °C. In the same way, the band at 1,710 cm^{-1} is the C=C mode of the HC=CH_2 vinyl group present in the polymer. One band at 1,610–1,625 cm^{-1} is characteristic of the δ(O–H) bending mode.

Magnetic measurements It is difficult to determine from FTIR spectra the concentration of impurities. For this purpose, magnetic measurements should be done to characterize the material. We have already reviewed the magnetic properties of $LiFePO_4$ and reported how to proceed with the analysis of the data to identify the impurities and determine their concentration [42]. We guide the reader to this review for the details. For simplicity, we exclude from this section the $LiFeP_2O_7$ impurity that is antiferromagetic and is quite easily detected by FTIR. All the other Fe-based impurities met in $LiFePO_4$ are either ferromagnetic (Fe_2P) or ferrimagnetic ($Li_3Fe_2(PO_4)_3$, γ-Fe_2O_3). In both cases, they come out under the form of nano-sized particles that carry a macroscopic magnetic moment below the ordering temperature. In their ferro- or ferri-magnetic ordered phase, these impurities are then easily spin-polarized by the application of an external magnetic field H. This is in contrast to pure $LiFePO_4$, since this material is an antiferromagnet with the Néel temperature T_N=50 K [2]. Therefore, the magnetization curves M as a function of the field H show, at low field, a nonlinear behavior due to the superparamagnetic contribution of the impurity particles. At higher field where the external component is saturated, the linear behavior is recovered, with the slope equal to the magnetic susceptibility of pure $LiFePO_4$. The ordering temperature of the impurities is thus easily determined as the temperature at which this nonlinear component at low field takes place. From the measurement of the magnetization curves $M(_H)$ at different temperatures, it is then straightforward to identify the impurities by their ordering temperature, 26 K for NASICON, 150 K for Fe_2P, above room temperature in the case of γ-Fe_2O_3. This behavior is illustrated in Fig. 6. The fraction of iron involved in the impurities can also be determined, together with the size of the impurity particles, from the fit of the magnetization curves, in a simple model of superparamagnetism [43]. This control of the impurities has progressively made possible the adjustment of the different synthesis parameters to get rid of all of them. We have already mentioned that Fe_2P is observed if the sample is prepared at temperature T_s> 750 °C; NASICON and $LiFeP_2O_7$ in the case where the sintering temperature (°C) was too low; and actually, all of them are systematically detected if hydrogen is not present in the synthesis process. The reason is that iron "likes" to be in the trivalent state. The synthesis being performed at temperature much too low for any carbothermal reduction of Fe, the reduction to Fe^{2+} oxidation state in $LiFePO_4$ is insured by hydrogen. That is why the carbon precursor used for the carbon coating process is always an organic compound, i.e., a compound that contains both H and C atoms. The carbon liberated during the sintering is used to make the carbon coating; the gaseous hydrogen compounds liberated during the process are the reducing agents [41]. However, this propensity for Fe^{3+} oxidation makes necessary the control of the impurities in $LiFePO_4$, and the combination of FTIR and magnetic experiments is the tool to control the quality of the product concerning this aspect.

Fig. 6 **a** Magnetization curves of a sample poisoned with γ-Fe_2O_3. The nonlinear part of the magnetization at low field exists already at room temperature since the magnetic ordering temperature of this impurity is very high. **b** Magnetization curves of a sample poisoned with Fe_2P; the onset of strong nonlinearity at small field is now limited to the range of temperatures smaller than the Curie temperature of this impurity, 150 K. **c** The $Li_3Fe_2(PO_4)_3$ impurity that poison this sample is best evidenced on the M/H (T) curve at H=10 kOe, by the anomaly at 26 K where the this impurity undergoes a weak first-order transition to a ferromagnetic phase

There is one impurity that does not contain iron: Li_3PO_4. This impurity is generated when an excess of Li is present among the precursors during the synthesis; it can be detected and quantified by XRD and inductive coupling plasma (ICP) analyses [44]. This impurity is not an advantage for electrochemical applications since Li_3PO_4 is an inert mass. However, the impact is limited to a loss of capacity per gram of product in the mass ratio between $LiFePO_4$ and Li_3PO_4. On the other hand, if $LiFePO_4$ is prepared with a Li deficiency, the XRD analysis gives evidence of an increase of the electron density on lithium positions of the olivine lattice, which can be attributed to the presence of iron ions on Li sites. This is actually much more damaging to the electrochemical performance since an iron ion on a Li site can block the channel of Li ions where it is located. Both the XRD and the ICP analyses show that the resulting product in such a case is a homogeneous solution of composition $Li_{1-2x}Fe_xFePO_4$ [44]. This formula shows that the intrinsic defect associated to the Li-deficiency

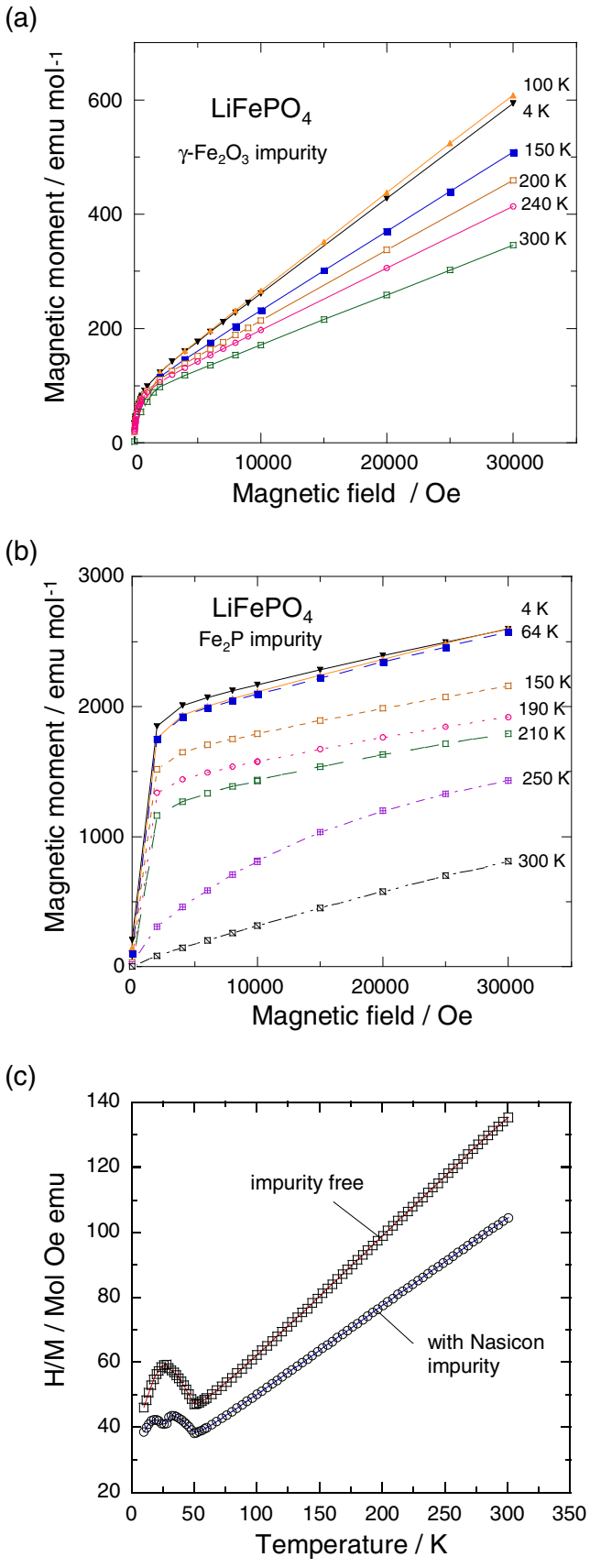

is a complex made of one Fe^{2+} ion on a Li^{+} site plus a Li vacancy. In the Kröger–Vink notation, this defect is thus $Fe^{\bullet}_{Li}+V'_{Li}$. The presence of Fe on a Li site has previously been observed in samples prepared by the hydrothermal route when the temperature T_s chosen for the synthesis is lower than 200 °C [45, 46]. Yet, the limit of solubility for this complex defect is only $x_c \approx 0.06$. Beyond this limit, the defects precipitate, resulting in the formation of $Fe_3(PO_4)_2$ as an impurity phase, observed by XRD and ICP analysis [44].

Storage conditions: sensitivity to moisture

When a company has made the quality controls along the lines described above, it has the ability to produce $LiFePO_4$ with the required performance for the most demanding uses. This step was reached a few years ago. Nevertheless, the feedback of the manufactures making batteries to the chemical industries that prepared such a $LiFePO_4$ product was controversial. This difference of appreciation at this last step obviously was due to a different history of the $LiFePO_4$ powder between the exit of the chemical company that made it and the integration of the powder in a battery element. It was soon realized that the problem came from the storage conditions [47]. $LiFePO_4$ is not sensitive to the oxygen of air; however, it is sensitive to moisture. The reactivity of the material to H_2O has been investigated by immersion of the product in water [47, 48] or simply by exposure of the particle to the humidity of the atmosphere [48, 49]. Unfortunately, the carbon layer is of no help and does not protect the particles against humidity. In presence of H_2O molecules, the lithium in the 3-nm thick surface layer is extracted from the particle, and reacts with H_2O to form LiOH first, and then combines with CO_2 in ambient atmosphere to form Li_2CO_3. Both of them are detected by Raman spectroscopy [48]. This surface contamination is damageable to the electrochemical properties, as it can be seen in Fig. 7. On the other hand, the delithiated surface layer forms an $FePO_4$ film that constitutes a waterproof coat, so that the material is actually much less sensitive to humidity than the lamellar compounds, for instance [49, 50]. Nevertheless, Fig. 7 shows that storage in dry chamber 5% humidity is mandatory (and sufficient) to keep the product with its full abilities.

Trends in the research on the olivine family

Now that $LiFePO_4$ can be prepared at an industrial scale with optimized properties, the efforts are now focused on other aspects that may hinder the development of electric or hybrid vehicles. One is the price of the product. In a Li-ion battery, the price of the cathode enters as about 30% of the price of the battery and is thus by far the most costly element. To reduce the price, the lower limits of the sintering temperature (°C) and

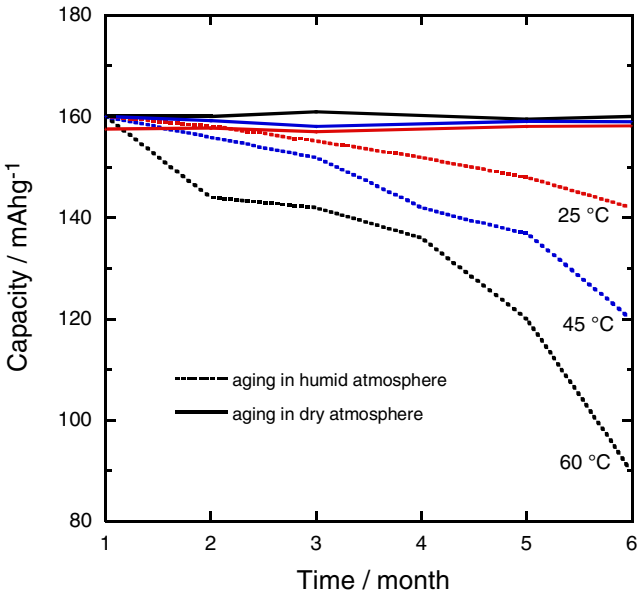

Fig. 7 Capacity of the C-$LiFePO_4$ (HTR sample)/$LiPF_6$-EC-DEC/Li cells as a function of time spent in dry atmosphere and in ambient atmosphere (55% relative humidity), at three different temperatures. The temperatures at which the full curves (in dry atmosphere) have been obtained (in color in the web version) can be distinguished by the fact that they do not overlap and the property that the lower the temperature, the higher the capacity is

of the time spent for the carbon coating process have been determined [18]. The reduction of the price may also be achieved by a less expensive synthesis process, like the preparation from the molten state [51], which makes possible the synthesis of particles of any size down to *circa* 20 nm. This decrease in the size of the particles is of interest to gain power. Li-ion batteries built with this small grain size, and $Li_4Ti_5O_{12}$ anode have been tested over 30,000 cycles without significant aging, even at deep charge and discharge in 5 min [52]. Note, however, that this outstanding gain in power has been possible only by replacing graphite by $Li_4Ti_5O_{12}$ in the anode. This is at the expense of the energy density, because the voltage of the battery is decreased by the potential of $Li_4Ti_5O_{12}$ vs. Li^0/Li^+, which is 1.5 V. This is just an example of the general trend in Li-ion batteries: one has to choose between more power and more energy, depending on the use that is targeted.

The energy density of $LiFePO_4$ is about 560 Wh kg^{-1}. Since it is quite close to the theoretical value, increasing the energy density of the cathode element means switching to another compound. $LiCoPO_4$ and $LiNiPO_4$ have a higher voltage (4.8 and 5.1 V, respectively, vs. Li^0/Li^+), which exceeds the stability window of the electrolytes presently available. $LiMnPO_4$ has a smaller voltage 4.1 eV, which makes it attractive, because this voltage is still within the electrolyte window and larger than that of $LiFePO_4$. However, the electric conductivity of $LiMnPO_4$ is even smaller than that of $LiFePO_4$. Therefore, the same recipes that were successful to overcome this problem in $LiFePO_4$ have been attempted in the case of $LiMnPO_4$. First, decrease the size of the particles to decrease the path length of electrons inside the material. Different synthesis routes have made possible the preparation of well-crystallized powders with a size of the order of 50 nm: solid-state reaction in molten hydrocarbon [53], polyol synthesis [54, 55], and spray pyrolysis plus ball milling [56]. Second, coat the particles with conductive carbon. Unfortunately, the carbon is less reactive with Mn than with Fe, and the carbon coating of $LiMnPO_4$ turns out to be much more difficult than that of $LiFePO_4$. Many efforts have been made to prepare C-$LiMnPO_4$ particles [57–59]. The price to obtain an initial discharge capacity in the range 130–140 mAh g^{-1} at C/10 rate was to immerse the $LiMnPO_4$ in important quantities of carbon, namely in the range 20 wt.% [60] to 30% [56, 61]. However, the amount of carbon in a commercial lithium-ion battery should not exceed a

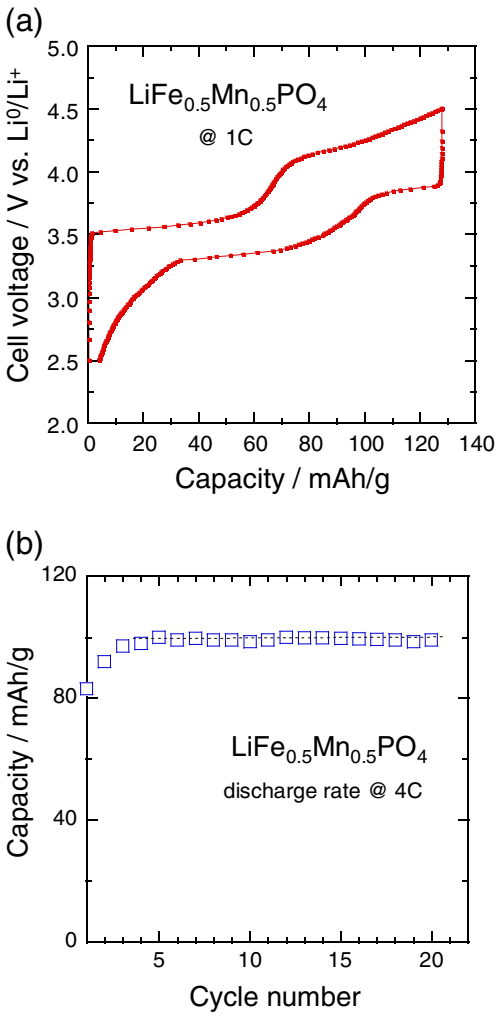

Fig. 8 **a** Voltage profile of Li/$LiPF_6$-EC–DEC/$LiFe_{0.5}Mn_{0.5}PO_4$ cell. The charge–discharge process was carried out at the 1 C rate (170 mAh g^{-1}). **b** Cycle life of $LiFe_{0.5}Mn_{0.5}PO_4$ cathode at discharge rate 4 C

few percent, and at such low concentrations, the capacity is smaller [62] and the material contains Li_3PO_4 impurity acting as an inert mass. Therefore, new routes have been tried. Since the methods applied to $LiFePO_4$ cannot be extrapolated directly to $LiMnPO_4$, to the point where the performance of $LiMnPO_4$ is not competitive with $LiFePO_4$, the first idea was to study the solid solution $LiMn_xFe_{1-x}PO_4$ to investigate which intermediate composition is the best compromise to take advantage of the Mn^{2+}/Mn^{3+} redox potential, 4.1 V vs. Li^0/Li^+, without losing too much in the cycling life and power [63]. Indeed, the extraction and insertion of Li proceed at two steps at 3.4 and 4.1 V, as the iron ions are reduced before the manganese ions [63–65]. Since then, carbon-coated $LiMn_xFe_{1-x}PO_4$ has been prepared successfully by different techniques [66–71], and the electrochemical properties are now well known. The electrochemical properties strongly decrease at $x \geq 0.8$ [68]. At these large Mn concentrations, the lattice cannot afford the strains induced by the valence change of Mn, as Mn^{3+} is a Jahn–Teller ion that generates local distortions in the lattice. The intermediate concentration $x=$ 0.5–0.6 turns out to be a good compromise. The same tools as the ones we have described in the previous section for $LiFePO_4$ have been used to characterize the solid solution at these intermediate concentrations, namely magnetic experiments [64, 65, 68], FTIR experiments [65, 71], Raman spectroscopy for the carbon coat [71], in addition to the conventional structural analyses including XRD and electron microscopy. As shown in Fig. 8, the capacity of C–$LiMn_{0.5}Fe_{0.5}PO_4$ at rate 1C is 130 mAh g^{-1}, still close to that of $LiFePO_4$, and even at rate 4C, the electrochemical reversibility is maintained; in addition, the cycle fading even at high current is remarkably small, at least for the 20 first cycles where it has been tested [65].

To bypass the limitation in the Fe/Mn ratio of the solid solutions, a new route has been explored recently [72]. $LiMnPO_4$ particles have been coated with $LiFePO_4$. Then, it is possible to coat this composite with carbon, by taking advantage of the fact that this deposit on $LiFePO_4$ is easily performed. Now the product is a composite with a core region of $LiMnPO_4$ surrounded by a coat of $LiFePO_4$; conductive carbon forms the surface layer [72]. The TEM image of such a particle is shown in Fig. 9 for the case where the particle contains a concentration of Mn twice that of Fe. The electrochemical properties have been measured and compared with those of the solid solution with the same Mn/Fe ratio, namely C-$LiMn_{2/3}Fe_{1/3}PO_4$ with the same size of the particles, namely 0.1–0.2 μm. For the C–$LiFePO_4$–$LiMnPO_4$ composite material, at C-rate C/24, the initial capacity is 119.3 mAh g^{-1}, with a ratio discharge/charge D/C close to unity. At 10C, the delivered capacity is 65.5 mAh g^{-1}. For a sample $LiMn_{2/3}Fe_{1/3}PO_4$ with the same size of particles and the same carbon coating, the capacity of the first charge at C/24 is only 54.5 mAh g^{-1} and the delivered capacity at 10 C is only 23.3 mAh g^{-1}. The composite has thus a much better performance.

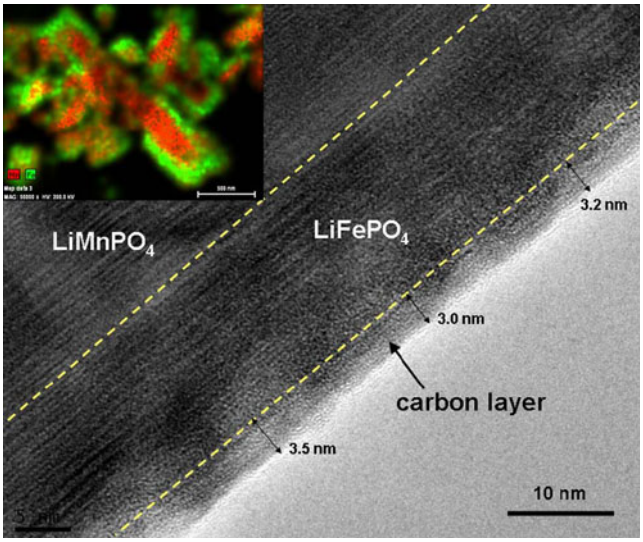

Fig. 9 TEM image of C-$LiFePO_4$-$LiMnPO_4$ showing the different layers of a particle of this composite. The EDX image demonstrates that $LiFePO_4$ forms a continuous layer on the surfaces of $LiMnPO_4$ particles

Concluding remarks

The $LiFePO_4$ material has major advantages: it is not toxic; its thermal stability is remarkable, it ranks number one in terms of safety and power. It is then not surprising that it is winning the market for hybrid and electric vehicles across the world. However, this olivine material may somehow be a victim of its success. The manufacturing of $LiFePO_4$ is in rapid expansion in an increasing number of companies, selling on the market products that have the same label of iron phosphate, but are not the same, and actually range from bad to good. The ability of the product to fulfill the expectations as a cathode element for demanding applications such as electric transportation relies on the quality control that is mandatory and it includes different tools that have been reviewed. The consequence is a product that may not be cheap, but this is the price to pay to get a reproducible and optimized product needed for a battery with very long cycling life and very high power. New synthesis routes are expected to reduce the price. The progress in the preparation of more elaborate composite materials with other members of the family opens a route to use other members of the olivine family to increase the voltage, and thus the energy density. The research on the olivine family will continue to be as active as it has always been since the pioneering work of John Goodenough.

References

1. von Fuchs JN (1834) Über ein neues mineral (triphylin). J für Praktische Chem 3:98–104
2. Santoro RP, Newnham RE (1967) Antiferromagnetism in $LiFePO_4$. Acta Cryst 22:344–347
3. Iakubovich OV, Simonov MA, Belov NV (1977) Crystal structure of triphyline $LiFePO_4$. Doklady Akad Nauk 235:93–95
4. Streltsov VA, Belokoneva EL, Tsirelson VG, Hansen NK (1993) Multipole analysis of the electron density in triphylite $LiFePO_4$, using X-ray diffraction data. Acta Cryst B 49:147–153
5. Padhi AK, Nanjundaswamy KS, Goodenough JB (1997) Phospho-olivines as positive-electrode materials for rechargeable lithium batteries. J Electrochem Soc 144:1188–1194
6. Julien CM, Mauger A, Zaghib K (2011) Surface effects on electrochemical properties of nano-sized $LiFePO_4$. J Mater Chem 21:9955–9968
7. Delacourt C, Laffont L, Bouchet R, Wurm C, Leriche JB, Morcette M, Tarascon JM, Masquelier C (2005) Toward understanding of electrical limitations (electronic, ionic) in $LiMPO_4$ (M=Fe, Mn). J Electrochem Soc 152:A913–A921
8. Zhou F, Kang K, Maxisch T, Ceder G, Morgan D (2004) The electronic structure and band gap of $LiFePO_4$ and $LiMnPO_4$. Solid State Comm 132:181–186
9. Zaghib K, Mauger A, Goodenough JB, Gendron F, Julien CM (2007) Electronic, optical, and magnetic properties of $LiFePO_4$: small magnetic polaron effects. Chem Mater 19:3740–3747
10. Murawski L (1982) Electrical conductivity in iron-containing oxide glasses. J Mater Sci 17:2155–2163
11. Murawski L, Barczynski RJ, Samatowicz D (2003) Electronic conductivity in Na_2O–FeO–P_2O_5 glasses. Solid State Ionics 157:293–298, and references therein
12. Huang H, Yin SC, Nazar LF (2001) Approaching theoretical capacity of $LiFePO_4$ at room temperature at high rates. Electrochem Solid State Lett 4:A170–A172
13. Zaghib K, Striebel K, Guerfi A, Shim J, Armand M, Gauthier M (2004) $LiFePO_4$/polymer/natural graphite: low cost Li-ion batteries. Electrochim Acta 50:263–270
14. Ravet N, Chouinard Y, Magnan JF, Besner S, Gauthier M, Armand M (2001) Electroactivity of natural and synthetic triphylite. J Power Sourc 97–98:503–507
15. Bewlay SL, Konstantinov K, Wang GX, Dou SX, Liu HK (2004) Conductivity improvements to spray-produced $LiFePO_4$ by addition of a carbon source. Mater Lett 58:1788–1791
16. Hsu KF, Tsay SY, Hwang BJ (2004) Synthesis and characterization of nano-sized $LiFePO_4$ cathode materials prepared by a citric acid-based sol–gel route. J Mater Chem 14:2690–2695
17. Doeff MM, Hu Y, Mc Larnon F, Kostecki R (2003) Effect of surface carbon structure on the electrochemical performance of $LiFePO_4$. Electrochem Solid State Lett 6:A207–A209
18. Trudeau ML, Laul D, Veillette R, Serventi AM, Zaghib K, Mauger A, Julien CM (2011) In-situ HRTEM synthesis observation of nano-structured carbon coated $LiFePO_4$. J Power Sourc 196:7383–7394
19. Kostecki R, Schnyder B, Alliata D, Song X, Kinoshita K, Kotz R (2001) Surface studies of carbon films from pyrolyzed photoresist. Thin Solid Films 396:36–43
20. Hu Y, Doeff MM, Kostecki R, Finones R (2004) Electrochemical performance of sol–gel synthesized $LiFePO_4$ in lithium batteries. J Electrochem Soc 151:A1279–A1285
21. Julien CM, Zaghib K, Mauger A, Massot M, Ait-Salah A, Selmane M, Gendron F (2006) Characterization of the carbon coating onto $LiFePO_4$ particles used in lithium batteries. J Appl Phys 100:063511–063518
22. Massot M, Zaghib K, Mauger A, Gendron F, Julien CM (2007) Characterization of the carbon coating of $LiFePO_4$ by transmission electron microscopy and Raman spectroscopy. Mater Res Soc Symp Proc 972:AA13-7
23. Gaberscek M, Dominko R, Jamnik J (2007) Is small particle size more important than carbon coating? An example study of $LiFePO_4$. Electrochem Commun 9:2778–2783
24. Chen G, Song X, Richardson TJ (2007) Metastable solid-solution phases in the $LiFePO_4$/$FePO_4$ system. J Electrochem Soc 154: A627–632
25. Chen G, Song X, Richardson TJ (2006) Electron microscopy study of the $LiFePO_4$ to $FePO_4$ phase transition. Electrochem Solid State Lett 9:A295–A298
26. Ramana CV, Mauger A, Gendron F, Julien CM, Zaghib K (2009) Study of the Li-insertion/extraction process in $LiFePO_4$/$FePO_4$. J Power Sourc 187:555–564
27. Corce F, d'Epifanio A, Assoun J, Deptula A, Olczac T, Scrosati B (2002) A novel concept for the synthesis of an improved $LiFePO_4$ lithium battery Cathode. Electrochem Solid State Lett 5:A47–A50
28. Kim C, Park J, Lee K (2006) Effect of Fe_2P on the electron conductivity and electrochemical performance of $LiFePO_4$ synthesized by mechanical alloying using Fe^{3+} raw material. J Power Sourc 163:144–150
29. Liu Y, Cao C, Li J, Xu X (2010) Novel synthesis of Fe_2P–$LiFePO_4$ composites for Li-ion batteries. J Appl Electrochem 40:419–425
30. Zaghib K, Mauger A, Goodenough JB, Gendron F, Julien CM (2009) $LiFePO_4$: from material science to application as a positive electrode for Li-ion batteries. In: Garche J (ed) Encyclopedia of electrochemical power sources, five-volume set. Elsevier, Amsterdam
31. Chung SY, Bloking JT, Chiang YM (2002) Electronically conductive phospho-olivines as lithium storage electrodes. Nat Mater 1:123–128
32. Ellis BL, Wagenmaker M, Mulder FM, Nazar LF (2010) Comment on "Aliovalent substitutions in olivine lithium iron phosphate and impact on structure and properties". Adv Funct Mater 20:186–188
33. Islam MS, Driscoll DJ, Fischer CA, Slater PR (2005) Atomic-Scale Investigation of defects, dopants, and lithium transport in the $LiFePO_4$ olivine-type battery material. Chem Mater 17:5085–5092
34. Fisher CAJ, Prieto VMH, Islam MS (2008) Lithium Battery Materials $LiMPO_4$ (M=Mn, Fe, Co, and Ni): Insights into defect association, transport mechanisms, and doping behavior. Chem Mater 20:5907–5915
35. Wagenmaker M, Ellis BL, Lützenkirchen-Hecht D, Mulder FM, Nazar LF (2008) Proof of supervalent doping in olivine $LiFePO_4$. Chem Mater 20:6313–6315
36. Ravet N, Abouimrane A, Armand M (2003) On the electronic conductivity of phospho-olivines as lithium storage electrodes. Nat Mater 2:702–702
37. Herle PS, Ellis B, Coombs N, Nazar LF (2004) Nano-network electronic conduction in iron and nickel olivine phosphates. Nat Mater 3:147–152
38. Morgan D, Ven AVD, Ceder G (2004) Li Conductivity in Li_xMPO_4 (M=Mn, Fe, Co, Ni) olivine materials. Electrochem Solid State Lett 7:A30–A32
39. Nishimura SI, Kobayashi G, Ohoyama K, Kanno R, Yashima M, Yamada A (2008) Experimental visualization of lithium diffusion in Li_xFePO_4. Nat Mater 7:707–711
40. Paques-Ledent MT, Tarte P (1974) Vibrational studies of olivine-type compounds II orthophosphates, arsenates and vanadates $A^{I}B^{II}X^{V}O_4$. Spectrochimica Acta Part A 30:673–689
41. Ravet N, Gauthier M, Zaghib K, Mauger A, Goodenough JB, Gendron F, Julien CM (2007) Mechanism of the Fe^{2+} reduction at low temperature, for $LiFePO_4$ synthesis from a polymer additive. Chem Mater 19:2595–2602
42. Julien CM, Mauger A, Ait-Salah A, Massot M, Gendron F, Zaghib K (2007) Nanoscopic scale studies of $LiFePO_4$ as cathode material in lithium-ion batteries for HEV application. Ionics 13:395–411

43. Ait-Salah A, Mauger A, Julien CM, Gendron F (2006) Nano-sized impurity phase in relation with the mode of preparation of $LiFePO_4$. Mater Sci Eng B 129:232–244
44. Axmann P, Stinner C, Wohlfahrt-Mehrens M, Mauger A, Gendron F, Julien CM (2009) Nonstoichiometric $LiFePO_4$: defects and related properties. Chem Mater 21:1636–1644
45. Yang S, Zavajil PY, Whittingham MS (2001) Hydrothermal synthesis of lithium iron phosphate cathodes. Electrochem Commun 3:505–508
46. Chen J, Whittingham MS (2006) Hydrothermal synthesis of lithium iron phosphate. Electrochem Commun 8:855–858
47. Porcher W, Moreau P, Lestriez B, Jouanneau S, Le Cras F, Guyomard D (2008) Stability of $LiFePO_4$ in water and consequence on the Li battery behaviour. Ionics 14:583–587
48. Zaghib K, Dontigny M, Charest P, Labrecque JF, Guerfi A, Kopec M, Mauger A, Gendron F, Julien CM (2008) Aging of $LiFePO_4$ upon exposure to H_2O. J Power Sourc 185:698–710
49. Martin JF, Yamada A, Kobayashi G, Nishimura SI, Kanno R, Guyomard D, Dupré N (2008) Air exposure effect on $LiFePO_4$. Electrochem Solid State Lett 11:A12–A16
50. Zhang X, Jiang WJ, Zhu XP, Mauger A, Julien CM, Qilu R (2011) Aging of $LiNi_{1/3}Mn_{1/3}Co_{1/3}O_2$ cathode material upon exposure to H_2O. J Power Sourc 196:5102–5108
51. Zaghib K, Charest P, Dontigny M, Guerfi A, Lagacé M, Mauger A, Kopek M, Julien CM (2010) LiFePO4: from molten ingot to nanoparticles with high rate performance in Li-ion batteries. J Power Sourc 195:8280–8288
52. Zaghib K, Dontigny M, Guerfi A, Charest P, Rodrigues I, Mauger A, Julien CM (2011) Safe and fast-charging Li-ion battery with long shelf life for power applications. J Power Sourc 196:3949–3954
53. Choi D, Wan D, Bae LT, Xiao J, Nie Z, Wang W, Viswanathan VV, Lee YJ, Zhang JG, Graff GL, Yang Z, Liu J (2010) $LiMnPO_4$ nanoplate grown via solid-state reaction in molten hydrocarbon for Li-ion battery cathode. Nano Lett 10:2799–2805
54. Wang D, Buqa H, Crouzet M, Deghenghi G, Drezen T, Exnar I, Kwon N-H, Miners JH, Poletto L, Grätzel M (2009) High-performance, nano-structured $LiMnPO_4$ synthesized via a polyol method. J Power Sourc 189:624–628
55. Martha K, Markovski B, Grinblat J, Gofer Y, Haik O, Zinigrad E, Aurbach D, Drezen T, Wang D, Deghenghi G, Exnar I (2009) $LiMnPO_4$ as an advanced cathode material for rechargeable lithium batteries. J Electochem Soc 156:A541–552
56. Oh SM, Oh SW, Yoon CS, Scrosati B, Amine K, Sun YK (2010) High-performance carbon-$LiMnPO_4$ nanocomposite cathode for lithium batteries. Adv Funct Mater 20:3260–3265
57. Kuroda S, Tobori N, Sakuraba M, Sato Y (2003) Charge–discharge properties of a cathode prepared with ketjen black as the electro-conductive additive in lithium ion batteries. J Power Sourc 119–121:924–928
58. Xing W, Qiao SZ, Ding RG, Li F, Lu GQ, Yan ZF, Cheng HM (2006) Superior electric double layer capacitors using ordered mesoporous carbons. Carbon 44:216–224
59. Bakenov Z, Taniguchi I (2010) $LiMg_xMn_{1-x}PO_4$/C Cathodes for lithium batteries prepared by a combination of spray pyrolysis with wet ball milling. J Electrochem Soc 157:430–436
60. Bakenov Z, Taniguchi I (2005) Electrochemical performance of nanostructured $LiM_xMn_{2-x}O_4$ (M=Co and Al) powders at high charge–discharge operations. Solid State Ionics 176:1027–1034
61. Oh SM, Jung HG, Yoon CS, Myung ST, Chen ZH, Amine K, Sun YK (2011) Enhanced electrochemical performance of carbon-$LiMn_{1-x}Fe_xPO_4$ nanocomposite cathode for lithium-ion batteries. J Power Sourc 196:6924–6928
62. Oh SM, Oh SW, Myung ST, Lee SM, Sun YK (2010) The effects of calcination temperature on the electrochemical performance of $LiMnPO_4$ prepared by ultrasonic spray pyrolysis. J Alloy Comp 506:372–376
63. Yamada A, Chung S-C (2001) Crystal chemistry of the olivine-type $LiMn_yFe_{1-y}PO_4$ and $Mn_yFe_{1-y}PO_4$ as possible 4 V cathode materials for lithium batteries. J Electrochem Soc 148:A960–967
64. Yamada A, Takei Y, Koizumi H, Sonoyama N, Kanno R, Itoh K, Yonemura M, Kamiyama T (2006) Electrochemical, magnetic, and structural investigation of the $Li_x(Mn_yFe_{1-y})PO_4$ olivine phases. Chem Mater 18:804–813
65. Zaghib K, Mauger A, Gendron F, Massot M, Julien CM (2008) Insertion properties of $LiFe_{0.5}Mn_{0.5}PO_4$ electrode materials for Li-ion batteries. Ionics 14:371–376
66. Nakamura T, Sakumoto K, Okamoto M, Seki S, Kobayashi Y, Takeuchi T, Tabuchi M, Yamada Y (2007) Electrochemical study on Mn^{2+}-substitution in $LiFePO_4$ olivine compound. J Power Sourc 174:435–441
67. Molenda J, Ojczyk W, Marzec J (2007) Electrical conductivity and reaction with lithium of $LiFe_{1-y}Mn_yPO_4$ olivine-type cathode materials. J Power Sourc 174:689–694
68. Kopec M, Yamada A, Kobayashi G, Nishimura S, Kanno R, Mauger A, Gendron F, Julien CM (2009) Structural and magnetic properties of $Li_xMn_yFe_{1-y}PO_4$ electrode materials for Li-ion batteries. J Power Sourc 189:1154–1163
69. Bramnik NN, Bramnik KG, Nikolowski K, Hinterstein M, Baehtz C, Ehrenberg H (2005) Synchrotron diffraction study of lithium extraction from $LiMn_{0.6}Fe_{0.4}PO_4$. Electrochem Solid State Lett 8: A379–A381
70. Bini M, Mozzati MC, Galinetto P, Capsoni D, Ferrari S, Grandi MS, Massarotti V (2009) Structural, spectroscopic and magnetic investigation of the $LiFe_{1-x}Mn_xPO_4$ (x=0–0.18) solid solution. J. Solid State Chem 182:1972–1981
71. Yoncheva M, Koleva V, Mladenov M, Sendova-Vassileva M, Nikolaeva-Dimitrova M, Stoyanova R, Zhecheva E (2011) Carbon-coated nano-sized $LiFe_{1-x}Mn_xPO_4$ solid solutions ($0 \le x \le 1$) obtained from phosphate–formate precursors. J Mater Sci 46:7082–7089
72. Zaghib K, Trudeau M, Guerfi, A, Trottier J, Mauger A, Julien CM (2012) New advanced cathode material: $LiMnPO_4$ encapsulated with $LiFePO_4$. J Power Sources (in press)